



HAL
open science

Solid-State NMR/Dynamic Nuclear Polarization of Polypeptides in Planar Supported Lipid Bilayers

Evgeniy S. Salnikov, Hiba Sarrouj, Christian Reiter, Christopher Aisenbrey, Armin Porea, Fabien Aussenac, Olivier Ouari, Paul Tordo, Illya Fedotenko, Frank Engelke, et al.

► **To cite this version:**

Evgeniy S. Salnikov, Hiba Sarrouj, Christian Reiter, Christopher Aisenbrey, Armin Porea, et al.. Solid-State NMR/Dynamic Nuclear Polarization of Polypeptides in Planar Supported Lipid Bilayers. Journal of Physical Chemistry B, 2015, 119 (46), pp.14574 - 14583. 10.1021/acs.jpccb.5b07341 . hal-01424945

HAL Id: hal-01424945

<https://hal.science/hal-01424945v1>

Submitted on 19 Feb 2025

HAL is a multi-disciplinary open access archive for the deposit and dissemination of scientific research documents, whether they are published or not. The documents may come from teaching and research institutions in France or abroad, or from public or private research centers.

L'archive ouverte pluridisciplinaire **HAL**, est destinée au dépôt et à la diffusion de documents scientifiques de niveau recherche, publiés ou non, émanant des établissements d'enseignement et de recherche français ou étrangers, des laboratoires publics ou privés.



Distributed under a Creative Commons Attribution 4.0 International License

Solid-state NMR / Dynamic Nuclear Polarization of polypeptides in planar supported lipid bilayers

Evgeniy S. Salnikov¹, Hiba Sarrouj^{1,2}, Christian Reiter², Christopher Aisenbrey¹,
Armin Pureau², Fabien Aussenac³, Olivier Ouari⁴, Paul Tordo⁴, Illya Fedotenko⁴,
Frank Engelke^{2*}, and Burkhard Bechinger^{1*}

¹Institute of Chemistry, University of Strasbourg / CNRS, UMR7177, 67070 Strasbourg, France;

²Bruker BioSpin, Silberstreifen, 76287 Rheinstetten, Germany;

³Bruker BioSpin, 34, rue de l'Industrie, 67166 Wissembourg, France

⁴Aix Marseille Université, CNRS, Institut de Chimie Radicalaire, UMR 7273, 13013 Marseille, France.

* corresponding authors:

Burkhard Bechinger, Institut de chimie, 4, rue Blaise Pascal, 67070 Strasbourg, France

Tel.: + 33 3 68 85 13 03; FAX: + 33 3 68 85 17 35; E-mail: bechinge@unistra.fr

and

Frank Engelke, Bruker BioSpin, Silberstreifen, 76287 Rheinstetten, Germany

Tel.: +4972151616129; FAX: +49721516191129; E-mail: Frank.Engelke@bruker.com

ABSTRACT

Dynamic Nuclear Polarization has been developed to overcome the limitations of the inherently low signal intensity of NMR spectroscopy. This technique promises to be particularly useful for solid-state NMR spectroscopy where the signals are broadened over a larger frequency range and most investigations rely on recording low gamma nuclei. To extend the range of possible investigations a triple-resonance flat-coil solid-state NMR probe is presented with microwave irradiation capacities allowing the investigation of static samples at temperatures of 100K including supported lipid bilayers. The probe performance allows for two-dimensional separated local field experiments with high-power Lee-Goldberg decoupling and cross polarization under simultaneous irradiation from a gyrotron microwave generator. Efficient cooling of the sample turned out essential for best enhancements and line shape and needed the development of a dedicated cooling chamber. Furthermore, the geometry of supported membranes was optimized not only for good membrane alignment, handling, stability and filling factor of the coil but also for heat and microwave dissipation. Enhancement factors of 17-fold were obtained and a two-dimensional PISEMA spectrum of a transmembrane helical peptide was obtained in less than 2 hours.

ABBREVIATIONS USED

CP	cross polarization
DNP	dynamic nuclear polarization
EPR	electron paramagnetic resonance
HDPE	high-density polyethylene
LT	low temperature
MAS	magic angle sample spinning
NMR	nuclear magnetic resonance
P/L	peptide-to-lipid ratio
POPC	1-palmitoyl-2-oleoyl- <i>sn</i> -glycero-3-phosphocholine
PTFE	polytetrafluorethylene
RF	radio frequency
RT	room temperature

Solid-state NMR spectroscopy is a powerful method for the structural investigation of membrane polypeptides and has provided valuable information about the conformation, topology and dynamics in lipid bilayer environments. Two fundamentally different approaches have been developed for the structural investigation of biological macromolecules, namely magic angle sample spinning (MAS) and oriented solid-state NMR, which both have been used to determine important structural and dynamic features from uniformly or selectively labeled membrane proteins.¹⁻⁸

The latter approach consists in orienting membranes with respect to the magnetic field direction and exploiting the large anisotropies of the chemical shifts, dipolar and quadrupolar couplings that are obtained from such aligned samples.⁹ This technique has been successful in the structural analysis of, for example the transmembrane peptides gramicidin A, Vpu, alamethicin and phospholamban (*e.g.* ^{2,10}) but has also been applied to other, larger and functionally more complex membrane proteins (*e.g.* ⁸). Oriented solid-state NMR has also been used to monitor structural changes, for example, of phospholamban when bound to the large SERCA protein.² Whereas for some polypeptides accurate structures have been determined,^{2,10,11} this approach also provides detailed information about the tilt and rotational pitch angles of membrane-inserted helices where it can follow even small changes (*e.g.* of 1°) in structure or topology.^{12,13} Combining distance constraints and angular constraints from oriented solid-state NMR has resulted in a refined structural analysis.^{1,2,8,11}

A major problem of these approaches remains the inherently low signal intensity of NMR spectroscopy which results in the necessity to investigate relatively large quantities of polypeptides. The problem is already apparent in solution-state NMR but pronounced in solid-state NMR spectroscopy where the line width is larger and concomitantly the signal-to-noise reduced (assuming the same signal integral). In particular, in oriented samples in many cases the peptides as a whole or individual sites of a protein in phospholipid bilayers can exhibit an inherent and functionally important distribution of conformations and alignments which cause broad but highly informative line shapes,^{14,15} albeit other examples exist where much sharper signal intensities are observed.^{2,10,11}

In this context Dynamic Nuclear Polarization (DNP) techniques have been developed over the last decades^{16,17} and made commercially available recently.¹⁸ By transferring the large polarization of unpaired electrons via the irradiation of an EPR transition, a large signal to noise enhancement of the ¹H NMR signal can be achieved, with a theoretical maximum of 660 (γ_e/γ_n).

Although most studies using DNP in solid-state NMR experiments have been performed so far on samples rotating at the magic angle, the signal enhancements by DNP should be even more valuable for oriented membrane samples where the broad inherent line shapes make it more difficult to obtain reasonable signal-to-noise ratios and where additional experimental restraints result from the need to align the samples. Good sample alignment often requires to dilute the polypeptide in a lipid matrix (typically 1/50 to 1/200 mole/mole). Furthermore, much of the coil volume is occupied by the solid supports onto which the membranes are oriented,¹⁹⁻²¹ or by aqueous solution in order to comply with the particular conditions required to align bicellar systems.^{22,23}

However, it should be taken into consideration that DNP/solid-state NMR experiments are performed under very particular conditions, namely the possibility to irradiate the sample with microwaves of several Watts matching the EPR transitions at high magnetic fields (263 GHz for a 9.4 Tesla NMR magnet) and the need to slow down the relaxation rates of the unpaired electrons by keeping the sample at low temperatures.^{17,18,24} Therefore, best signal enhancements are obtained when the samples are cooled with liquid helium²⁴ or liquid nitrogen.^{17,18} It remains possible to perform DNP/solid-state NMR experiments also at increased, even ambient temperatures, but in these cases more modest enhancements are observed.^{25,26} In prior work we have therefore performed some proof-of-concepts studies to test if the technology can be applied to oriented membranes.^{27,28} With only MAS probes available at the time a lipid bilayer carrying a transmembrane model peptide labeled with ¹⁵N at one site was oriented on a polymer sheet, wrapped into a cylinder and investigated under low (around 1 kHz) and fast (8 KHz) MAS spinning conditions. The resulting ¹⁵N side-band intensities are indicative that the membranes remain oriented at 100K and under such MAS conditions up to 17-fold signal enhancements have been obtained when mixing bTbK or TOTAPOL biradicals into the oriented membranes.^{27,28}

Because a low temperature MAS probe for DNP/solid-state NMR was made available with the first commercial systems¹⁸ converting this probe for static measurements following previous flat-coil NMR probe developments²⁹ seems on first view straightforward. However, the geometries of oriented membrane samples result in a number of additional considerations.

First of all for the current three spin model of cross effect DNP the effect of MAS has been shown to be important in promoting the required mixing of direct product spin states.³¹ Sample spinning thereby helps in increasing the efficient DNP signal enhancements by the cross effect in frozen samples carrying biradicals.³⁰⁻³² As a consequence a larger fraction of the spins

become polarized under MAS and the signal enhancements obtained from static samples are several-fold decreased when compared to samples undergoing MAS in the optimal frequency range.^{18,32}

Second, the cooling gas arrives at the sample from one side and flows around the MAS rotor. At the same time the sample rotates quickly with the sample being close to the rotor walls. This helps in cooling the sample evenly. Notably, the better enhancements observed with sapphire when compared to zirconia rotors were associated with the better thermal conductivity of the latter illustrating the importance of homogenous cooling efficiency,³³ albeit the influence of the dielectric constant of the material and its wall thickness are also important and currently under investigation. In contrast, additional precautions have to be taken to assure a homogenous and efficient cooling of the static oriented samples which tend to also be relatively voluminous where the length exceeds the width and both are larger than their height.

Third, to be efficient the microwaves have to penetrate as much of the sample as possible. Once they leave the corrugated wave guide they have to pass the NMR coil to penetrate the sample. Importantly it has been shown that MAS rotors of appropriate thickness or the presence of dielectric particles in the sample helps to scatter and amplify the microwaves into the sample thereby assuring a more efficient sample irradiation.^{34,35} In contrast the oriented samples are usually only enveloped by plastic and Teflon wrapping, and in addition contain stacks of solid support and lipid bilayers with a repetition distance (typically 20-30 solid supports for a 3 mm stack) close to the wavelength of the microwaves (10^{-3} m). The effects of such an arrangement on the microwave penetration have so far not been investigated and tests of different sample geometries will be reported here.

MATERIALS AND METHODS

The phospholipid 1-palmitoyl-2-oleoyl-*sn*-glycero-3-phosphocholine (C16:0, C18:1-PC, POPC) is from Avanti Polar Lipids (Alabaster, AL). $^{15}\text{NH}_4\text{Cl}$ (99,5% ^{15}N) was purchased from Cambridge Isotope Laboratories (Andover, MA). All commercial material was used without further purification.

Peptide sequence and label positions. The hydrophobic peptide [$^{15}\text{N}_5$]- hΦ19W (KKKALLALLALAWALALLALLAKKK) was prepared by solid phase peptide synthesis as described previously.¹² At five subsequent positions leucine and alanine labeled with ^{15}N were incorporated into the peptide (underlined in the above sequence). The AMUPol and PyPol

biradicals were prepared as described previously.³⁶ The preparation and comparative evaluation of PyPol-C16, a derivative of PyPol bearing a palmitoyl chain, will be described in a separate paper discussing the effect of the polarizing agent structure on the signal enhancement in oriented experiments (Figure S1). The HRMS (ESI) analysis of the compound indicates an m/z of 906.6533 which compares well with the theoretical value of 906.6526 for $C_{49}H_{87}N_5O_{10} \bullet\bullet$ $[M+H]^+$.

Water/glycerol sample for DNP. A homogeneous mixture of 1.5 M $^{15}NH_4Cl$ and 10 mM AMUPol dissolved in $D_2O/H_2O/glycerol-d_8$ 30/10/60 by weight was placed in sapphire rotor and used as reference. The temperature dependence of the ^{15}N line width allows for temperature calibration (see Figure S2).

Membrane samples for DNP. A homogeneous mixture of lipid, peptide, and radical was obtained by co-dissolving the membrane components in trifluoroethanol. To prepare oriented-POPC membranes, the solution was spread onto ultra-thin cover glasses (3 x 8 mm for the DNP probe; 8 x 22 mm for conventional oriented solid-state NMR measurements; thickness 00; Marienfeld, Lauda-Konigshofen, Germany) or High-Density PolyEthylene (HDPE) film (3 x 8 mm, Goodfellow, Cambridge, UK), dried first in air and followed by high vacuum overnight.^{27,37} Thereafter, the sample was equilibrated during a day in an atmosphere of 93% relative humidity of D_2O/H_2O (90/10 by volume). The glass plates were then stacked on top of each other and wrapped in Teflon. The HDPE film with a sample was carefully folded to fit in the coil and flattened in between two sapphire plates of 3 x 8 mm and 0.5-0.8 mm thickness. In the case of non-oriented samples, the POPC suspension was transferred into the 3.2 mm sapphire rotor without mechanical support. The use of partially deuterated 'solvent' (lipid, water and glycerol) channels spin diffusion toward the protonated peptide chain.

DNP/solid-state NMR. DNP/solid-state NMR measurements were performed using a Bruker BioSpin wide-bore 9.4 T magnet and an Avance III solid-state NMR spectrometer equipped with a gyrotron producing 263 GHz irradiation, a microwave transmission line delivering about 5 W of microwave power at the sample (MAS probe), a cooling unit using liquid nitrogen and a low temperature triple resonance 3.2 mm MAS probe.¹⁸ The spectra shown in Fig. 3 were obtained using a commercial $^1H-^{13}C-^{15}N$ triple resonance MAS probe and setup for low temperatures of ≥ 100 K (Bruker, Wissembourg, France). An adiabatic CP pulse sequence³⁸ was used with a spectral width of 29.8 kHz and acquisition, cross polarization contact and recycle delay times of

8.6 ms, 0.3 ms and 3 s, respectively. The ^1H $\pi/2$ pulse and spinal64 heteronuclear decoupling field strengths B_1 corresponded to a nutation frequency of 50 kHz. To equilibrate the system before acquisition the sample was exposed to 16 dummy scans. An exponential line-broadening of 100 Hz was applied before Fourier transformation for membrane samples and no line-broadening in the case of water/glycerol. Spectra were externally referenced to $^{15}\text{NH}_4\text{Cl}$ powder at 40 ppm at room temperature.³⁹ The DNP signal enhancement was determined as a ratio in the integral signal intensity of MW ON versus MW OFF spectra obtained with identical parameters.

The oriented samples were investigated with a purposely built static solid-state NMR/DNP probe introduced in this paper. The PISEMA spectrum was recorded on 3.3mg [$^{15}\text{N}_5$]- h Φ 19W at a nominal temperature of 100K (where the actual sample temperature depends on the MW irradiation (~180K)). The peptide was reconstituted in a POPC membrane at a molar peptide-to-phospholipid ratio of 1/20 and oriented onto a HDPE film. The PyPol-C16 was added in the quantity of 0.2 mg per 20 mg of POPC membrane. A step-by-step protocol for setting up and analyzing the experiment are given in references^{19,40}. The effective B_1 field strength during the SEMA pulse train was 50 kHz. During the spin exchange period the amplitude of the ^1H B_1 field was decreased to 40.9 kHz to maintain the Hartmann– Hahn match condition with an effective field along the magic angle of 50 kHz.

RESULTS AND DISCUSSION

Probe design for static DNP/solid-state NMR

The probe used for the static DNP measurements is based on a Cryo-MAS probe equipped with a Dewar style shielding tube, vacuum jacked gas transfer line for sample cooling and a corrugated wave guide for microwave irradiation (Figure 1). The sample chamber and NMR coil are designed according to the requirements of the sample²⁹ and the conditions of the combined DNP and NMR experiments, namely reasonable cross polarization (CP) performance, proper cooling and microwave transparency.^{34,35}

The radiofrequency (RF) part of the probe consists of two channels connected to a free standing NMR coil with a 4 x 4 mm cross section and 10 mm length. In order to improve the microwave propagation through the RF coil, the 8.5 turns were wound with a variable pitch. The inter turn distance is 1.3 mm at the center and decreases symmetrically towards the coil endings.

As shown in Figure S3, the ^1H channel has a capacitive matching coupled to a tuning trimmer that is connected to the NMR coil via a transmission line. To isolate the ^1H frequency circuit from the Y-channel tuned to ^{15}N an LC-stop circuit is used. The Y-channel exhibits inductive matching and a tuning trimmer with ports for a shunt capacitor that enables the user to set the tuning range to the desired frequency band. The Y channel frequency is decoupled from the proton channel via grounding at the $\lambda/4$ point of the transmission line. The whole circuit as well as some representative sensitivity values and tuning ranges are illustrated in Figure S3. All trimmers used for this probe have polytetrafluorethylene (PTFE) dielectric and can be operated at cryogenic temperatures. A third channel (not shown in Fig. 1) for ^{13}C or ^{31}P has also been built into the circuit for future use.

In order to enable operation of the probe at temperatures close to 100K the probe is separated into two sections (see details in Fig. 1). The probe base with all the connectors and interfaces is held at room temperature or close to room temperature by heating foils at several positions. Two of them are there to keep warm the lower part of the microwave guide and another two are in contact with the walls of the probe base. In addition the probe base is flushed with dry nitrogen gas to keep it free of moisture and to avoid ice forming at the various feed-throughs leading into the cold part of the probe. The flushing gas also helps to distribute the heat and hence to smooth the temperature profile across the surface. For insulating the two probe sections a Vespel capsule with a thickness of approximately 30 mm is used with gas-tight feed-throughs for all mechanical actuators and RF-lines.

The sample chamber (Figure S4) is made of PTFE and surrounds the NMR coil with the sample. Two Teflon hoses are connected to the chamber guiding the cold gas from the transfer line outlet to the sample. In order to change the sample the chamber has to be disassembled.

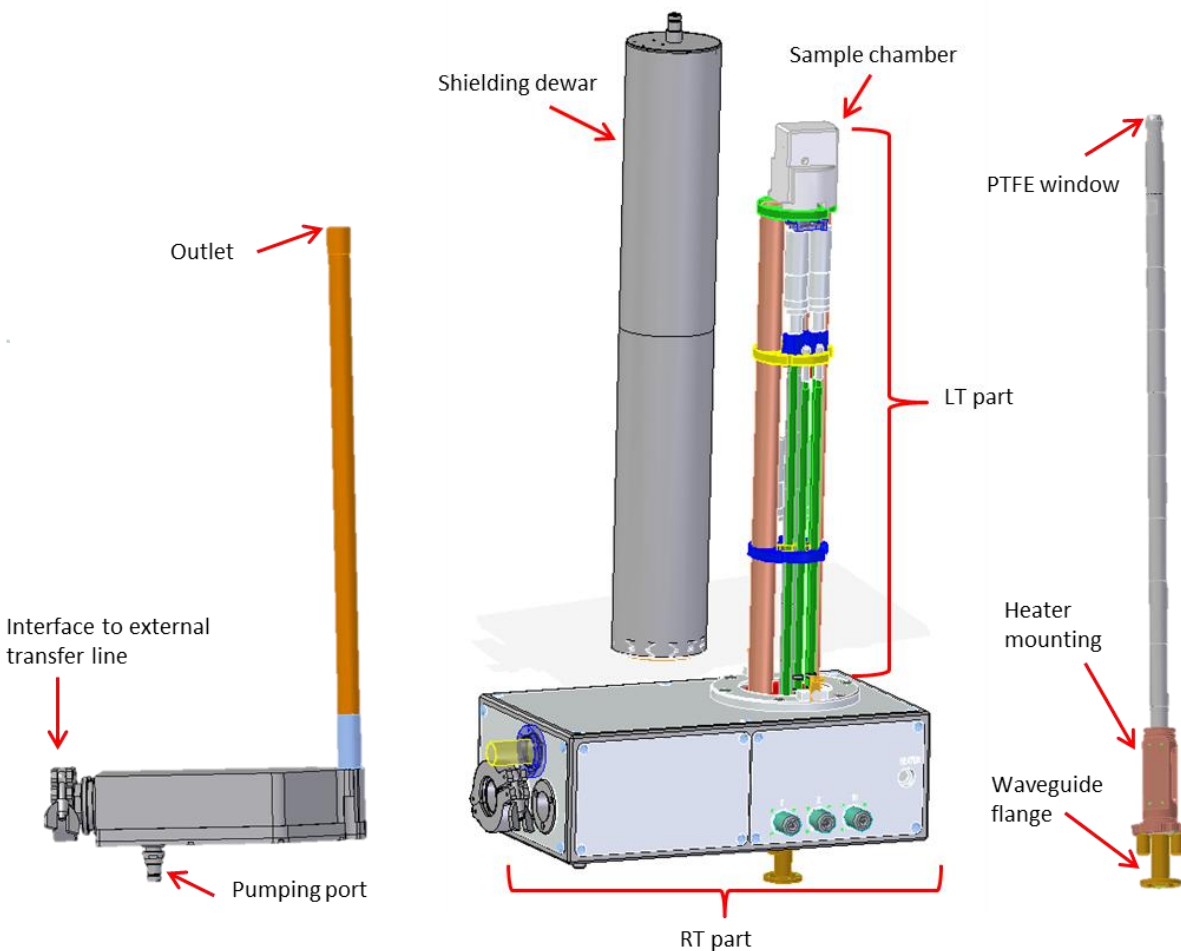


Figure 1: Left side: gas transfer line with ports; Center: complete probe with shielding Dewar; right side: waveguide (Graphics: Solid Edge ST6)

The low-temperature region of the probe is insulated from the magnet shim system by a double-wall evacuated shielding Dewar (Fig. 1 center). The sample chamber and all electronics are located inside this section. The cold gas is guided towards the sample chamber via three gas conducting channels inside a vacuum-insulated transfer line, the latter also enabling temperature regulation by means of channel heaters and PT100 temperature sensors. Two of the gas flows enter the sample chamber pointing onto the NMR-coil directly while the third one flushes the outer surface of the chamber. All three flows combine underneath the sample chamber and cool the RF electronics for increased sensitivity. Finally the gas flow leaves the probe through an exhaust pipe. Two thermocouples are used to read the temperature within the sample chamber and in the exhaust pipe respectively. The heat exchanger used to supply the cold nitrogen gas is a commercially available Bruker LT-MAS cooling cabinet.

Numerical analysis

Electromagnetic simulations at 263GHz were carried out using CST Microwave Studio 2014 (CST AG, Darmstadt, Germany) to study the field distribution in the sample. A geometrical model of the waveguide end, coil block, RF coil and sample stack was generated. Three sample geometries were studied: a sapphire rotor filled with a water/glycerol DNP sample serving as recreation of the reference sample, and two biomembrane stacks: one with glass as substrate and one with HDPE.

The glass stack consists of 20 glass layers of 0.1 mm thickness. Between each glass layer, a membrane layer of 0.065 mm width is inserted. Another layer of 0.1mm PTFE is added on the top and on the bottom of the stack.

The HDPE stack consists of 32 layers of 0.01 mm HDPE and 31 layers of membrane sample, again with a thickness of 0.065 mm. On the bottom, a Sapphire layer of 0.5 mm is added, and another one of 0.4 mm on the top. As in the case of the glass stack, a PTFE layer of 0.1 mm is added on top and bottom. The overall dimensions of both stacks are 10 mm x 2.4 mm x 3.435 mm.

Dielectric parameters of the various materials are set according to published data.^{34,41} For the bilayer sample, the dielectric parameters are taken from paraffin since a large part of the sample consists of lipids. A hexagonal mesh is used for spatial discretization. One or more cells are present in the direction of stacking to ensure that all material changes are adequately resolved. The cell dimensions are typically between 10 μm and 80 μm .

At the side of the waveguide opposing the coil, a waveguide port is placed and excited with an HE11 mode. The polarization angle can be set such that the E-field of the mode is either perpendicular (mode 1) or parallel (mode 2) to the coil windings. The simulations are carried out using the time-domain solver, and three-dimensional field data for the E and H fields is obtained. Cut views of the absolute H field distribution obtained in the stack samples are shown in Figure 2. The mean H field is analyzed in the sample material inside the coil and is converted to units of magnetic flux density B..

In the rotor reference sample, the mean B_{1S} field is 18.2 $\mu\text{T}/\sqrt{W}$ for mode 1 and 17.4 $\mu\text{T}/\sqrt{W}$ for mode 2. In the stacked biomembrane samples, the variation found between mode 1 and 2 is also less than 10%, but the mean field is higher in the stack with HDPE substrate. Compared to the mean field in the glass stack, it is 15% higher for mode 1 and 34%

higher for mode 2. In absolute numbers, the predicted B_{1S} field is 16-17 $\mu\text{T}/\sqrt{W}$ for the glass substrate and 20-22 $\mu\text{T}/\sqrt{W}$ for the HDPE substrate. It shall be noted that the absolute amount of bilayer sample is higher in the case of HDPE because the thickness of the support is 10-fold lower, such that more sample layers can be fitted into the sample stack.

The variation in mean field being less than 10% between excitation with mode 1 as opposed to mode 2 indicates that the coil is penetrable to the incident beam regardless of its polarization. Nevertheless, there is some variation in the field pattern. The presence of the stack leads to multiple reflections between the material boundaries, as well as diffraction, leading to inhomogeneous field patterns.

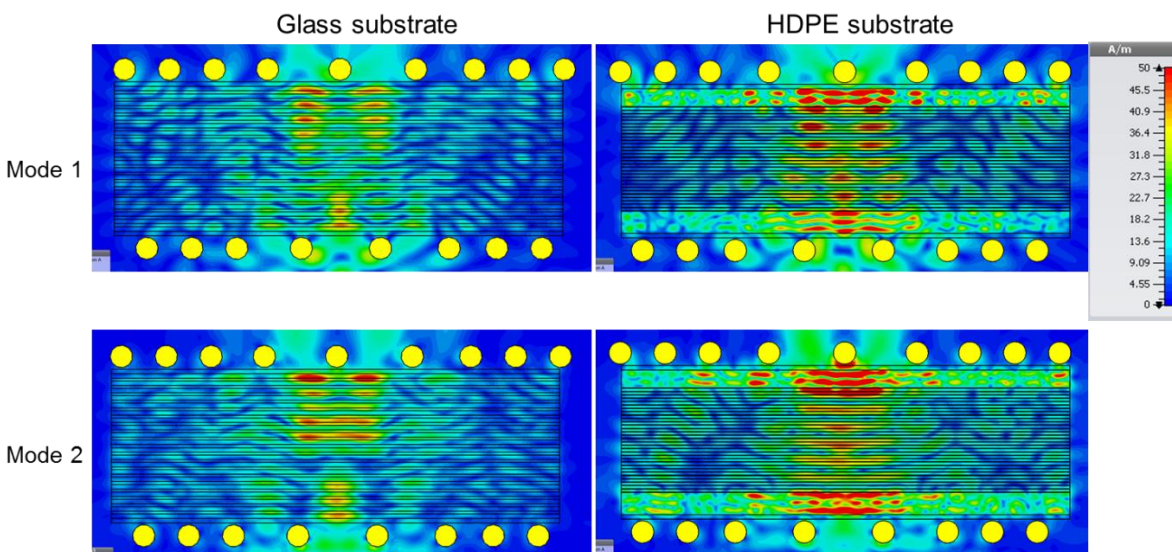


Figure 2: Central cut views through the sample stack showing the absolute H-field distribution (Graphics: CST Microwave Studio 2014)

Performance of the DNP/solid-state NMR Probe

In order to test RF performance of the static DNP probe shown in the Figures 1 and S3 with coil dimensions 4x4x10 mm the RF performance was measured with the goal to perform Lee-Goldberg decoupling and cross polarization as typically applied e.g. in separated local field experiments.⁴² In order to obtain B_1 fields of 50 kHz at 112K 19.1W were applied to the ^1H channel and at 125 W to the ^{15}N channel (measured on a glassy sample made from a solution of 1.5 M $^{15}\text{NH}_4\text{Cl}$ in glycerol/water with 10 mM AMUPOL). At room temperature 33.2 W and 235 W (solid $^{15}\text{NH}_4\text{Cl}$ powder), respectively, were required.

We then compared the static and the commercially available MAS 3.2 mm triple resonance solid-state NMR/DNP probes using two types of sample, namely a water /glycerol mixture (so called ‘DNP juice’) with AMUPOL as polarizing agent and a lipid membrane sample containing PyPol-C16 as polarizing agent (non oriented vesicles) both inside sapphire rotors. It should be noted that whereas these rotors remain truly static in the flat-coil probe they turn slowly (5 to 20 Hz) inside the MAS probe due to the incoming cooling gas. The ^1H - ^{15}N cross polarization experiments of the two samples exhibited DNP enhancement factors of 12 and 14, respectively, when the microwave on and off conditions are compared to each other (Fig. 3).

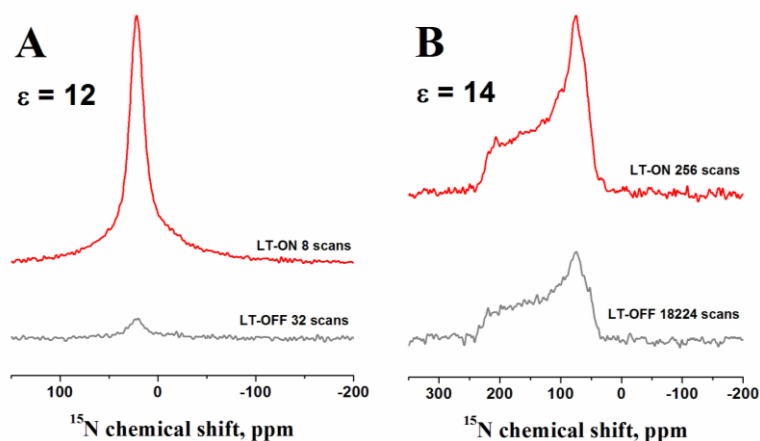


Figure 3: Proton-decoupled ^{15}N solid-state NMR spectra of 1.5 M $^{15}\text{NH}_4\text{Cl}$ in glycerol/water (“DNP juice”) / AMUPOL (panel A) and of ^{15}N -labelled peptide reconstituted into non-oriented membranes containing PyPol-C16 (panel B). Both samples were investigated in sapphire rotors placed into a 3.2 mm MAS probe. The ^{15}N spectra with MW ON (LT-ON) and OFF (LT-OFF) are shown. Spectra intensities were normalized to the noise level. The cooling gas causes residual spinning speeds in this “pseudo-static” mode of 5 Hz for the sample made of frozen DNP juice, and 20 Hz for the frozen membrane sample.

In the static probe similar enhancement factors were obtained for the sample made from DNP juice when the integrals of the resonance were analyzed. When the microwave intensity was increased by turning the current of the gyrotron from 20 mA to 40 mA a 17.5-fold enhancement of the peak height was transformed into a 25-fold increase. However, because at the same time the lines became narrower, the enhancement when analyzed from the integral of the resonances, was reduced from 12.3-fold at 20 mA to 10.5-fold at 40 mA (Table S1, Figure 4A). When the gyrotron current is further increased a decrease in both enhancements and line width are observed. In order to analyze these data in a more quantitative manner the line shape was correlated to changes in the temperature using a calibration curve obtained with the same sample

using the MAS probe (Figure S2). Notably, due to the microwave and RF irradiation the temperature at the sample may be higher as the one measured at the thermocouple which records the temperature of the gas outside the coil (Figure S4). Table S1a indicates the gradual increase in signal enhancement and temperature when the microwave power increases. However, when the glass melting temperature of $\sim 160\text{K}$ is nearly reached in the sample, the enhancement suddenly drops.

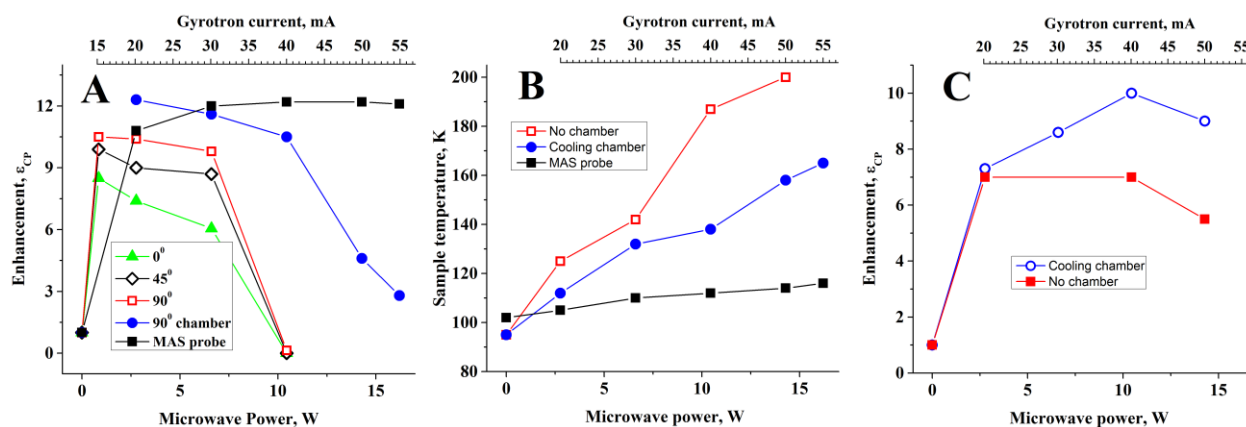


Figure 4: DNP enhancements as a function of microwave intensity for 1.5 M $^{15}\text{NH}_4\text{Cl}$ in glycerol/water (“DNP juice”) in the presence of AMUPOL (panels A and B) or for ^{15}N -peptide/membrane in the presence of PyPol-C16 (panel C). The samples were placed inside sapphire rotors in the static probe (Fig. 1). A. Experimentally measured enhancement as a function of the microwave power for three different coil orientations of the static probe with and without cooling chamber and comparison with the MAS probe in its static mode. B: Sample temperature in the static probe with and without cooling chamber. C: DNP enhancements (integral) obtained for the membrane sample with and without cooling chamber. The microwave power and the corresponding gyrotron currents are indicated. The signal enhancements are calculated from the integrals of the resonances.

Clearly an efficient cooling arrangement is essential for these experiments in order to carry away the high amount of heat induced by the microwaves. Upon an increase of microwave power by 5W an increase in temperature of about 20 K is observed with the cooling chamber, and this effect doubles when the sample chamber was removed (Fig. 4A,B). Because in this configuration the stream of cold gas is inefficient in cooling the sample, a sudden drop in DNP efficiency occurs already at 40 mA (corresponding to 10.5 W input power at the entry to the probe body). However, this ‘open arrangement’ allowed us to optimize the relative alignment of the incoming microwave polarization and the coil, which clearly varies significantly with the

relative orientation of the guide and the coil (Fig. 4A), in agreement with the simulations of the field distributions within the sample predicting more shielding in mode 1 (Fig. 2).

Notably, the experimentally obtained DNP enhancement varied between different orientations of the coil with respect to the incoming beam. For the 90° orientation, which corresponds to mode 1, a higher enhancement was found than for 0° orientation. This corresponds with the variation of the mean H field that was found from the electromagnetic simulations of the respective setup with the rotor sample, although the numerical results only showed a slight increase in mean field for mode 1. However, a quantitative comparison is difficult since a field distribution is obtained from the simulations, but enhancement is obtained from experiments. Furthermore, the enhancement is also a function of the temperature, which itself has been shown to change depending on the power of the beam.

DNP enhancements with non-oriented membrane samples

When non-oriented membrane samples (vesicle paste) inside a sapphire rotor (Fig. 3B) were investigated with the static DNP probe an enhancement factor of 10 was observed both at 20 mA and at 40 mA (Figure 4C, Table S2). In contrast to the ammonium chloride sample the temperature determination through the resonance line width as demonstrated in Figure S2 is not possible. However, under these conditions a collapse of the ¹H line width is observed upon microwave irradiation, suggesting that the membrane-associated water undergoes a phase transition. When the ¹H signal of this sample was analyzed as a function of temperature, a melting point for membrane-associated water was observed at > 240 K. Therefore, it is quite likely that sample heating is a reason for the lower DNP enhancement factor in the static probe ($\epsilon = 10$; Figure 4C, Table S2) when compared to the pseudo-static MAS probe ($\epsilon = 12$; Fig 4A). Indeed, the ¹H line shape suggests that even with the cooling chamber the microwave irradiation heats the sample in the static sapphire rotor to ~250K at 60 mA (Table S2). Furthermore, in a truly static mode the microwaves enter the sample from one side only, whereas slow turning of the sample should allow a more even penetration of microwaves as well as a more equal exposure to the cooling gas (which also enters in a directional manner). In this context it is noteworthy that fast MAS spinning at about 3 kHz has additional effects on the quantum transitions and results in several fold increased enhancement factors when compared to the ‘pseudo-static’ mode^{18,32} an

effect reproduced also in this work where enhancements of about 35-fold and about 100-fold are observed for the membrane and the reference sample made from ‘DNP juice’ (Figure S6).

Optimizing the preparation of supported lipid bilayers for alignment and DNP

In a next step membranes oriented along mechanical supports were prepared. In order to test DNP efficiency and signal alignment two different approaches were chosen. First the samples were applied onto ultra-thin glass plates, a protocol that is well established at room temperature where the solid support provides well-aligned phospholipid bilayers.³⁷ Second, polymer films have been used to prepare oriented samples²⁰ also for magic angle oriented sample spinning (MAOSS) experiments⁴³ including for our very first DNP/solid-state NMR experiments on oriented membranes.²⁷ These materials are more flexible and therefore special precautions have to be taken during preparation and handling of the oriented bilayers. Here we used two thin sapphire plates to support the sample configuration. The experimental set-up is sketched in Figure 5.

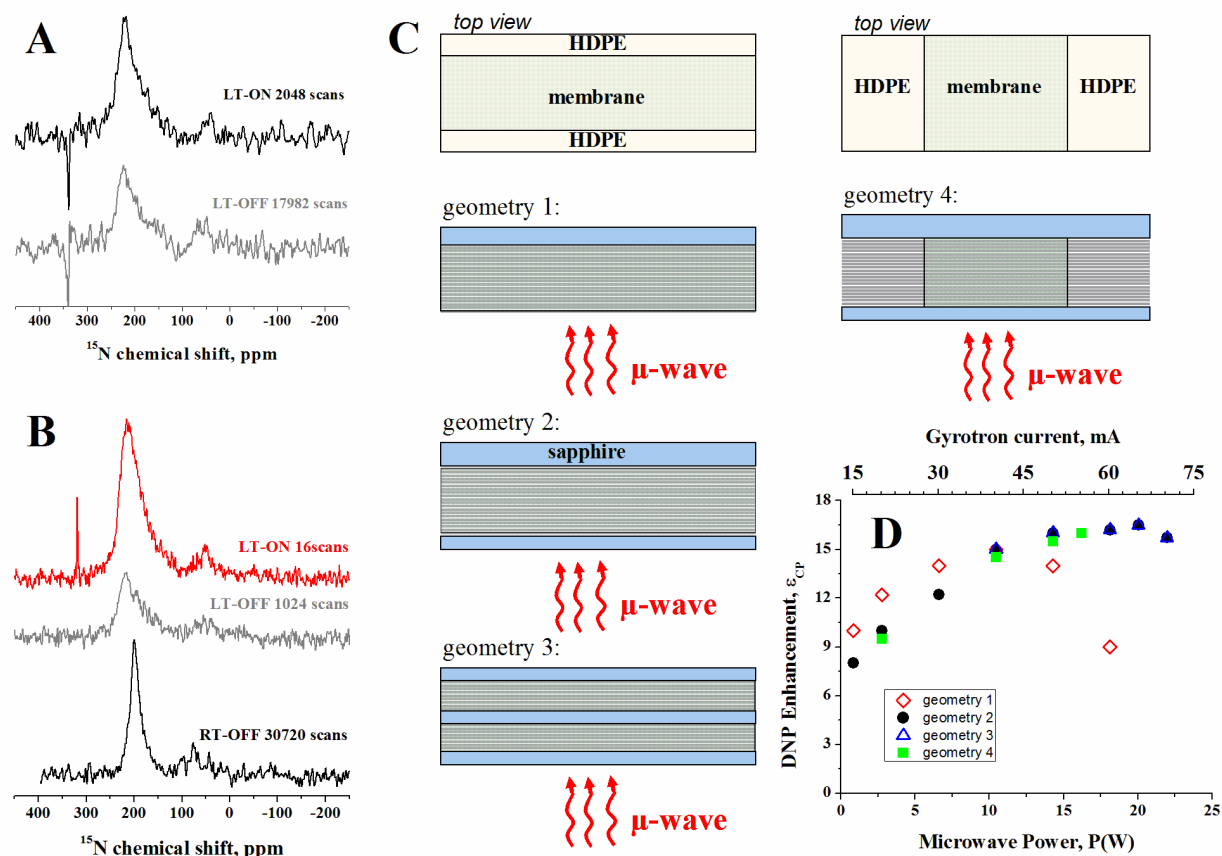


Figure 5. Proton-decoupled ^{15}N -cross polarization spectra of $[\text{}^{15}\text{N}_5]\text{-h}\Phi\text{19W}$ in POPC with PyPol-C16 biradical oriented on glass plates (A; DNP enhancement 4.3-fold at 2.8 W (20mA) microwave power) or on HDPE film (B; enhancement 16.5 at 20 W (65mA), sample geometry 2). The spectra are shown with the normalized noise level and obtained with different number of scans. LT-ON is for the cryo-temperatures under MW irradiation; LT-OFF is for the cryo-temperatures without MW irradiation and RT-OFF is for the room temperature spectrum. C. Illustration of different sample geometries obtained with the polyethylene (HDPE) films and D. the corresponding DNP enhancements as a function of microwave power.

The enhancement is considerably better when the HDPE stacks were investigated. This is probably due to the thermal insulation of the glass, which prevents the heat produced by the microwaves to be conducted efficiently to the surface of the sample where it can be cooled by the gas stream. As a consequence, at a gyrotron current of 40 mA the ^1H lines of these samples collapse, suggesting that temperatures $\geq 240\text{ K}$ are reached within the sample. For related reasons sapphire MAS rotors have been found to be better suited for DNP efficiency than those made from zirconium.³³ When the membranes on HDPE stabilized by sapphire plates were investigated, enhancements of 16.5 were obtained with a gyrotron current of 65 mA. The measurement of the same sample at room temperature (see RT-OFF spectrum in Fig.5B) gives the line-width of 900Hz (which is considerably narrower than 2200Hz line-width at cryo temperature and indicates motional averaging) and signal-to-noise of 15.6 after 30720 scans at room temperature (2s recycle delay). On the other hand the signal-to-noise of 17.6 was obtained after 16 scans (less than 1 minute) under DNP conditions. I.e. the experimental time-save is on the level of ~ 1630 , which transforms into the DNP signal enhancement of 40-fold when compared to the room temperature measurements.

It should be noted that the enhancements obtained here cannot directly be compared to those in DNP/MAS solid-state NMR experiments for several reasons. First, the samples here are truly static samples where enhancement factors 5-10 times below those obtained under MAS conditions are observed, as sample spinning helps in the polarization transfer between electrons and nuclei.^{18,32} Second, MAS probably also helps in cooling/irradiating the sample more uniformly. Third, most of the work on biradicals has aimed to optimize the conditions for glasses made of solutions where the biradicals distribute in a homogenous manner. This is not as easy to achieve in matrix-free samples⁴⁴ including oriented lipid bilayers where the biradicals tested so far tend to accumulate at the membrane interface.²⁸ Therefore, first attempts to improve the biradical distribution have been made for example by anchoring the biradicals in a more

controlled manner to the lipid bilayer.⁴⁵⁻⁴⁷ The Pypol-C16 shows indeed improved enhancement in membrane environments over other biradicals tested by us before^{27,28} and its synthesis and properties will be discussed in a comparative manner elsewhere.

The sapphire plates not only stabilize the HDPE stacks but they may also help in propagating the microwaves and cooling the sample.^{34,35} Therefore we tested different geometrical arrangements where we varied the number of sapphire supports as well as the localization of the oriented membranes relative to the incoming microwaves (Figs. 4A and 5).

The different geometries for the sample packing are shown in Figure 5C. The sample with the membrane paste concentrated in the center of the NMR coil (geometry 4) and the sample with the membrane distributed along the full length (8mm) of the plates (geometry 2) showed no difference in the enhancement factor suggesting that microwave irradiation is distributed equally within the membrane samples in both cases. Sample geometry 3 exhibits the same enhancement as observed with arrangements 2 and 4 which indicates that the additional dielectric interfaces do not promote microwave dissipation in the same manner as previously observed with dielectric crystalline particles of ~0.4mm size.³⁵ However, it is possible that dissipation on planar rather than irregular/curved surfaces may have different effects and/or that the presence of several HDPE layers, each 0.01 mm thick, may already result in dielectric dissipation thus that the additional sapphire plate makes only a minor difference. When the sapphire plate facing the microwave beam is absent a sudden drop in enhancement is observed when the gyrotron currents reach 40 mA. This suggests that the sapphire plates shield and/or better scatter the microwaves as well as the heat produced by this irradiation.

Finally, the NMR probe was tested for its performance on a two-dimensional separated local field spectrum where the resolution in the dipolar dimension is enhanced by phase- and frequency switched Lee-Goldberg decoupling of the homonuclear ¹H interactions when at the same time cross polarized with the ¹⁵N nucleus.⁴² The spectrum obtained at 100 K and under DNP conditions has been obtained in less than 2 hours (Figure 6) whereas it takes days under standard conditions at room temperature. It is enough to say that despite of relatively narrow lines reasonable signal-to-noise level of 7.9 was obtained after 50 minutes of acquisition from much bigger sample containing 10mg of [¹⁵N₅]- hΦ19W using E-free probe. The time save has a factor of 316 and therefore the signal enhancement under MW is on the level of 18-fold. This model peptide is highly dynamic and at room temperature a relatively sharp peak is obtained, but the five resonances collapse in a single unresolved intensity (not shown). At the low temperature the

different conformational and orientational states of the peptide are frozen which results in a broadened line shape (see Fig.S7). Nevertheless the helical wheel can be discerned allowing the analysis of the tilt angle. Whereas here the purpose is to test our probe and DNP conditions for this type of spectroscopy, optimizing the spectral resolution of the sample is out of scope. With the short acquisition times the latter can be achieved by testing different temperatures (to test the effect of motional averaging) for example by optimizing the gyrotron power against enhancement and resolution as well by varying the cooling efficiency. In addition it has been shown that the peptide homogeneity and spectral resolution are also dependent on the membrane lipid composition.^{48,49} Notably, because different conformational and topological states are trapped under the cryogenic temperatures of oriented DNP / solid-state NMR conditions, the approach probably works best for polypeptide sequences that are characterized by a rigid packing and uniform conformational features.^{50,51}

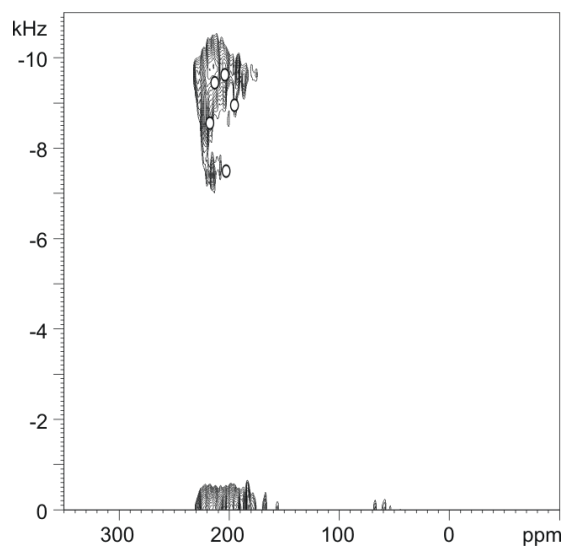


Figure 6: DNP / solid-state PISEMA spectrum of the transmembrane model peptide [$^{15}\text{N}_5$]-h Φ 19W carrying five consecutive ^{15}N labels (3.3 mg) reconstituted into 20 mg uniaxially oriented POPC bilayers (P/L =1/20 mole/mole) at a nominal temperature of 100K (actual sample temperature \sim 180K) in the presence of 200 μg PyPol-C16. The DNP enhancement is 16-fold. The dots indicate a simulation of chemical shift/dipolar couplings of the five labeled sites for an ideal helix ($\Phi = -64^\circ$, $\Psi = -41^\circ$) at tilt angle 10° . The simulation was performed with Simpson,⁵² which used the main tensor values 218/79/60 ppm and 9.9 kHz for the N-H coupling.⁵³

In conclusion, a triple-resonance flat-coil solid-state NMR probe with microwave irradiation capacities was assembled which allows DNP/solid-state NMR experiments of static samples at temperatures of 100K. The probe performance allows for two-dimensional separated local field experiments with high-power Lee-Goldberg decoupling and cross polarization under simultaneous irradiation from a gyrotron microwave generator. Importantly, efficient cooling of the sample, which needed to be optimized against the microwave input proved essential for best enhancements and line shape. The geometry of supported lipid bilayers encompassing a labeled membrane polypeptide (uniaxially oriented membranes) was optimized taking into consideration membrane alignment, heat intake, handling, stability and filling factor of the coil. A first two-dimensional PISEMA spectrum of a transmembrane helical peptide was obtained in less than 2 hours. The shortening of acquisition times by orders of magnitude should make two- and three dimensional solid-state NMR experiments routinely accessible also for oriented membrane samples⁵⁴. Additional improvements will be possible with new biradicals, different lipid compositions and further optimized sample preparation protocols especially designed for oriented membrane systems.

ACKNOWLEDGMENTS

We are grateful to Melanie Rosay, Werner Maas and Alain Belguise for continuous support and discussions as well as for making available time at the DNP instrument. We also acknowledge the technical help by Delphine Hatey during peptide synthesis and preparation. The grant by the CNRS and Buker Biospin, France to fund the PhD position of H.S. has been a great encouragement to us. Furthermore the financial contributions of the Agence Nationale de la Recherche (projects ProLipIn 10-BLAN-731, membraneDNP 12-BSV5-0012 and the LabEx Chemistry of Complex Systems 10-LABX-0026_CSC), the University of Strasbourg, the CNRS, the Région Alsace and the RTRA International Center of Frontier Research in Chemistry are gratefully acknowledged.

REFERENCES

- (1) Hong, M.; de Grado, W. F. *Protein Sci* **2012**, *21*, 1620.
- (2) Gustavsson, M.; Verardi, R. et al. *Proc Natl Acad Sci USA* **2013**, *110*, 17338.

- (3) Baker, L. A.; Baldus, M. *Curr Opin Struc Biol* **2014**, *27*, 48.
- (4) Ong, Y. S.; Lakatos, A. et al. *J Am Chem Soc* **2013**, *135*, 15754.
- (5) Eddy, M. T.; Andreas, L. et al. *Biochemistry* **2015**, *54*, 994.
- (6) Gattin, Z.; Schneider, R. et al. *J Biomol NMR* **2014**.
- (7) Linke, D.; Shahid, S. et al. *Faseb J* **2013**, *27*.
- (8) Das, N.; Dai, J. et al. *Proc Natl Acad Sci U S A* **2015**, *112*, E119.
- (9) Bechinger, B.; Sizun, C. *Concepts Magn Res* **2003**, *18A*, 130
- (10) Cross, T. A. *Methods in Enzymology* **1997**, *289*, 672.
- (11) Michalek, M.; Salnikov, E. et al. *Biophys J* **2013**, *105*, 699.
- (12) Aisenbrey, C.; Bechinger, B. *Biochemistry* **2004**, *43*, 10502.
- (13) Yamamoto, K.; H. N. Dürr, U. H. N. et al. *Sci Rep* **2013**, *3*, 2538 | DOI: 10.1038/srep02538.
- (14) Perrone, B.; Miles, A. J. et al. *Eur. Biophys J* **2014**, *43*, 499.
- (15) Aisenbrey, C.; Sudheendra, U. S. et al. *Eur Biophys J* **2007**, *36*, 451.
- (16) Can, T. V.; Caporini, M. A. et al. *J Chem Phys* **2014**, *141*.
- (17) Ni, Q. Z.; Daviso, E. et al. *Acc Chem Res* **2013**, *46*, 1933.
- (18) Rosay, M.; Tometich, L. et al. *Phys Chem Chem Phys* **2010**, *12*, 5850.
- (19) Aisenbrey, C.; Michalek, M. et al. In *Lipid-Protein Interactions: Methods and Protocols*; Kleinschmidt, J. H., Ed.; Springer: New York, 2013, p 357.
- (20) Auge, S.; Mazarguil, H. et al. *J Magn Reson.* **1997**, *124*, 455.
- (21) Prosser, R. S.; Hunt, S. A.; Vold, R. R. *J Magn Reson Ser B* **1995**, *109*, 109.
- (22) Loudet, C.; Diller, A. et al. *Prog Lipid Res* **2010**, *49*, 289.
- (23) Prosser, R. S.; Hwang, J. S.; Vold, R. R. *Biophys J* **1998**, *74*, 2405.
- (24) Thurber, K. R.; Yau, W. M.; Tycko, R. *J Magn Reson* **2010**, *204*, 303.
- (25) Akbey, U.; Linden, A. H.; Oschkinat, H. *Appl Magn Reson* **2012**, *43*, 81.
- (26) Jaktetchai, O.; Denysenkoy, V. et al. *J Am Chem Soc* **2014**, *136*, 15533.
- (27) Salnikov, E.; Rosay, M. et al. *J Am Chem Soc* **2010**, *132*, 5940.
- (28) Salnikov, E. S.; Ouari, O. et al. *Appl Magn Reson* **2012**, *43*, 91.
- (29) Bechinger, B.; Opella, S. J. *J Magn Res* **1991**, *95*, 585.
- (30) Thurber, K. R.; Tycko, R. *J Chem Phys* **2014**, *140*.
- (31) Thurber, K. R.; Tycko, R. *J Chem Phys* **2012**, *137*, 084508.
- (32) Mentink-Vigier, F.; Akbey, U. et al. *J Magn Reson* **2012**, *224*, 13.
- (33) Lide, D. R. e. *Properties of Solids*; CRC Press: Boca Raton, FL, 2005.
- (34) Nanni, E. A.; Barnes, A. B. et al. *J Magn Reson* **2011**, *210*, 16.
- (35) Kubicki, D. J.; Rossini, A. J. et al. *J Am Chem Soc* **2014**, *136*, 15711.
- (36) Sauvee, C.; Rosay, M. et al. *Angew Chem Int Edit* **2013**, *52*, 10858.
- (37) Aisenbrey, C.; Bertani, P.; Bechinger, B. In *Antimicrobial Peptides* Guiliani, A., Rinaldi, A. C., Eds.; Humana Press, Springer: N.Y., 2010, p 209.
- (38) Hediger, S.; Meier, B. H.; Ernst, R. R. *Chem Phys Lett.* **1995**, *240*, 449.
- (39) Bertani, P.; Raya, J.; Bechinger, B. *Solid-state NMR spec.* **2014**, *61-62*, 15.
- (40) Salnikov, E.; Aisenbrey, C. et al. In *New Developments in NMR: Advances in Biological Solid-State NMR, Proteins and Membrane-Active Peptides*; Separovic, F., Naito, A., Eds.; Royal Society of Chemistry: 2014, p 214.
- (41) Lamb, J. W. *Int. J. Infrared and Millimeter Waves* **1996**, *17*, 1997.
- (42) Ramamoorthy, A.; Wei, Y.; Lee, D. *Ann Rep NMR Spec* **2004**, *52*, 1.
- (43) Sizun, C.; Bechinger, B. *J. Am. Chem. Soc.* **2002**, *124*, 1146.
- (44) Takahashi, H.; Lee, D. et al. *Angew Chem Int Edit* **2012**, *51*, 11766.
- (45) Mao, J. F.; Akhmetzyanov, D. et al. *J Am Chem Soc* **2013**, *135*, 19275.

- (46) Smith, A. N.; Caporini, M. A. et al. *Angew Chem Int Edit* **2015**, *54*, 1542.
- (47) Fernandez-de-Alba, C.; Takahashi, H. et al. *Chemistry* **2015**, *21*, 4512.
- (48) Lee, D. K.; Kwon, B. S.; Ramamoorthy, A. *Langmuir* **2008**, *24*, 13598.
- (49) Salnikov, E. S.; De Zotti, M. et al. *J Phys Chem B* **2009**, *113*, 3034.
- (50) Kamihira, M.; Vosegaard, T. et al. *J Struct. Biol* **2005**, *149*, 7.
- (51) Vogt, T. C. B.; Schinzel, S.; Bechinger, B. *J Biomol NMR* **2003**, *26*, 1.
- (52) Bak, M.; Rasmussen, J. T.; Nielsen, N. C. *J Magn Reson* **2000**, *147*, 296.
- (53) Salnikov, E.; Bertani, P. et al. *J Biomol NMR* **2009**, *45*, 373.
- (54) Gopinath, T.; Mote, K. R.; Veglia, G. *J Biomol NMR* **2015**.

TOC graphics:

